Performance Evaluation of CMIP6 Global Climate Models for Selecting Models for Climate Projection over Nigeria

Mohamed Sanusi Shiru
Seoul National University of Science and Technology
Eun-Sung Chung (eschung@seoultech.ac.kr)
Seoul National University of Science and Technology https://orcid.org/0000-0002-4329-1800

Research Article

Keywords: CMIP6, compromise programming, climate change, multi model ensemble, statistical indices, Nigeria

Posted Date: June 25th, 2021

DOI: https://doi.org/10.21203/rs.3.rs-642786/v1

Performance Evaluation of CMIP6 Global Climate Models for Selecting Models for Climate Projection over Nigeria

[1,2]Mohammed Sanusi Shiru, [1*]Eun-Sung Chung

[1]Department of Civil Engineering, Seoul National University of Science and Technology, 01811, Seoul, Republic of Korea.

[2]Department of Environmental Sciences, Faculty of Science, Federal University Dutse, P.M.B, 7156, Dutse, Nigeria.

*Corresponding Author: Dr. Eun-Sung Chung (eschung@seoultech.ac.kr)

Abstract

This study assessed the performances of 13 GCMs of the CMIP6 in replicating precipitation and maximum and minimum temperatures over Nigeria during 1984–2014 in order to identify the best GCMs for multi model ensemble aggregation for climate projection. The study uses the monthly full reanalysis precipitation product Version 6 of Global Precipitation Climatology Centre and the maximum and minimum temperature CRU version TS v. 3.23 products of Climatic Research Unit as reference data. The study applied five statistical indices namely, normalized root mean square error, percentage of bias, Nash-Sutcliffe efficiency, and coefficient of determination; and volumetric efficiency. Compromise programming (CP) was then used in the aggregation of the scores of the different GCMs for the variables. Spatial assessment, probability distribution function, Taylor diagram, and mean monthly assessments were used in confirming the findings from the CP. The study revealed that CP was able to uniformly evaluate the GCMs even though there were some contradictory results in the statistical indicators. Spatial assessment of the GCMs in relation to the observed showed the highest ranked GCMs by the CP were able to better reproduce the observed properties. The least ranking GCMs were observed to have both spatially overestimated or underestimated precipitation and temperature over the study area. In combination with the other measures, the GCMs were ranked using the final scores from the CP. IPSL-CM6A-LR, NESM3, CMCC-CM2-SR5, and ACCESS-ESM1-5 were the highest ranking GCMs for precipitation. For maximum temperature, INM.CM4-8, BCC-CSM2-MR, MRI-ESM2-0, and ACCESS-ESM1-5 ranked the highest while AWI-CM-1-1-MR, IPSL-CM6A-LR, INM.CM5-0, and CanESM5 ranked the highest for minimum temperature.

Keywords: CMIP6, compromise programming, climate change, multi model ensemble, statistical indices, Nigeria

1. Introduction

There have been many studies on the impacts of climate change resulting from increasing temperature and erratic precipitations in many parts of the globe (Iqbal et al., 2019; Khan et al., 2020a; Salman et al., 2020; Shiru et al., 2018). It has been commonly concluded that disaster frequencies, severities and risks, particularly relating to droughts and floods have increased (Alamgir et al., 2019; Asdak and Supian, 2018; Ayugi et al., 2020; Manawi et al., 2020). They are also expected to increase in the future under different emission scenarios of generations of global climate models (GCM) (Homsi et al., 2020; Sa'adi et al., 2019; Shiru et al., 2020c; Tan et al., 2020); which are the primary tools for climate predictions and future climate projections. For increased confidence in future climate projections, performance evaluation of GCMs is imperative (Zhao et al., 2020). Such evaluations are pivotal to the development of reliable adaptation and mitigation measures against the risks and impacts of climate change.

Over the years, there has been development of many GCMs for the different scenarios of the IPCC assessment reports including the coupled model inter-comparison project (CMIP) phase 3, phase 5, and the recently released phase 6. Many studies reported improvements of the CMIP5 over the CMIP3 (Tanveer et al., 2016; Taylor et al., 2012; Zhou et al., 2017). The main differences between the CMIP6 simulations and the earlier CMIP phases (CMIP3 and CMIP5) are the start years for the future scenarios, new sets of specifications for concentration, emission, and land-use scenarios (Gidden et al., 2019). Although the CMIP6 is yet to have the complete ensemble GCMs, some recent studies have demonstrated its robustness over CMIP5 in some regions e.g. South Asia (Zhai et al., 2020); China (Xin et al., 2020); South Korea (Song et al., 2020), Australia (Grose et al., 2020) and Africa (Ayugi et al., 2021a). It is therefore important to assess their performances in other regions where they are yet or have not been widely applied.

Because there has been a general consensus that all GCMs show similar climate characteristics over the globe, each GCM has been treated as an equal. However, there are variations in GCMs spatial performances across the globe (Chen et al., 2017; Homsi et al., 2020; Khan et al., 2020b). Therefore, many studies have recommended the aggregation of a multi-model ensemble (MME) from a pool of GCMs by excluding the GCMs that are considered the least realistic in order to reduce the uncertainties associated with the GCMs (Ahmed et al., 2019a; Lutz et al., 2016; Shiru et al., 2019a). Though the combination of multiple GCMs for projection is characterized by challenges such as the effectiveness of error cancellation from the averaging of GCMs, they are better than usage of a single model (Knutti et al., 2010). There is also the challenge of the definition of performance metrics which sufficiently relates to the models' prediction skills, and the issue of an overall model ranking method of multipurpose in models subset selection.

Studies have been conducted in assessing the performances of GCMs in many parts of the globe using different statistical measures (Rivera and Arnould, 2020; Sreelatha and Anand Raj, 2019). However, there can be challenges in decision making as to which GCMs performed best due to contradictions in the outputs from different statistical measures (Ayugi et al., 2021b; Klutse et al., 2021). This emphasizes the implementation of a compromise solution which can consider tradeoffs among the measures for selecting the best models.

Compromise programming (CP) (Zeleny, 1973) is one of the multi-criteria decision making techniques applied in many fields including climate studies. The basic idea in CP is to identify the ideal solution as a point where each considered attributes' achieves its optimum value. Hence, the ideal solution will be that point that is closest to the ideal point. Interference by decision making is prevented in CP through its ability in identifying the closest ideal solution (Rezaei et al., 2017; Samal and Kansal, 2015). In climate research, CP was used in compromising the various performances and selecting the best gridded precipitation data over Iraq (Salman et al., 2019) and in the ranking of GCMs (Ahmed et al., 2019b; Raju et al., 2017).

The CMIP6 being recently released is not known to have been applied in Nigeria. GCM selection over the region has also not been conducted using CP method. Therefore, this present study aims to select the most suitable GCMs from a total of 13 precipitation, and maximum and minimum temperatures for aggregation into MMEs for climate projection over the region. This study uses the monthly Global Precipitation Climatological Center (GPCC) precipitation and Climate Research Unit (CRU) maximum and minimum temperature data as reference data (observed data). Five statistical indices namely: normalized root mean square error (NRMSE), Percentage of Bias (Pbias), Nash-Sutcliffe Efficiency (NSE), Coefficient of Determination (R^2) and Volumetric Efficiency (VE) were used to identify the performances of CMIP6 relative to the observed precipitation and maximum and minimum temperatures. Using CP, the scores from the metrics were used for ranking of the GCMs. Probability distribution function (PDF) and Taylor diagram (TD) were used to assess the performances of the GCMs in replicating the observed data. The annual and monthly time series were also plotted to assess the closeness of the GCMs to the observed. Finally, the best performing GCMs were selected. So far, the study background and objectives of the study have been presented. Henceforth, section two presents the study area and datasets; section three presents the methodology, section four, the results, section five, the discussions, while the conclusions are given in section six.

2. Study Area and Datasets

2.1. Study Area

Nigeria in the western part of Africa (Latitudes $4^0 15'$ – $13^0 55'$ N; Longitude: $2^0 40'$ – $14^0 45'$E), covering an area of 923,000 km^2 (Figure 1) is considered for this study. In the north of the country is Niger, to the east are Chad and Cameroon, Benin Republic borders it at the west while the stretch of the southern part is bordered by the Atlantic Ocean. The country has two major seasons' namely rainy and dry seasons. The climate of the country varies spatial and temporally with the southern parts receiving over 2,000 mm annual precipitation during April - October, and below 500 mm precipitation in the northern parts occurring during June and September. In the inland areas of the country, mean annual minimum and maximum temperatures vary diurnally from 19.0–22.8°C and 32.3–36.0°C respectively. At the coasts of the country, mean annual minimum temperature ranges from 21.8–22.7°C while mean annual maximum ranges from 30.7–31.0°C. Different climatic conditions mainly: monsoon climate in the south, tropical savanna climate at the central and warm semi-arid and warm desert climate in the north exists in the country. The ecological zones within the country are Mangrove swamp and Rainforest in the south, Guinea savanna at the central, and Sudan savanna and Sahel savanna in the north. The lowest point within the country at 0 m is at the coastal south adjoined by the Atlantic Ocean while Chappal Waddi at 2,419 m in the northeastern part of the country is the highest point.

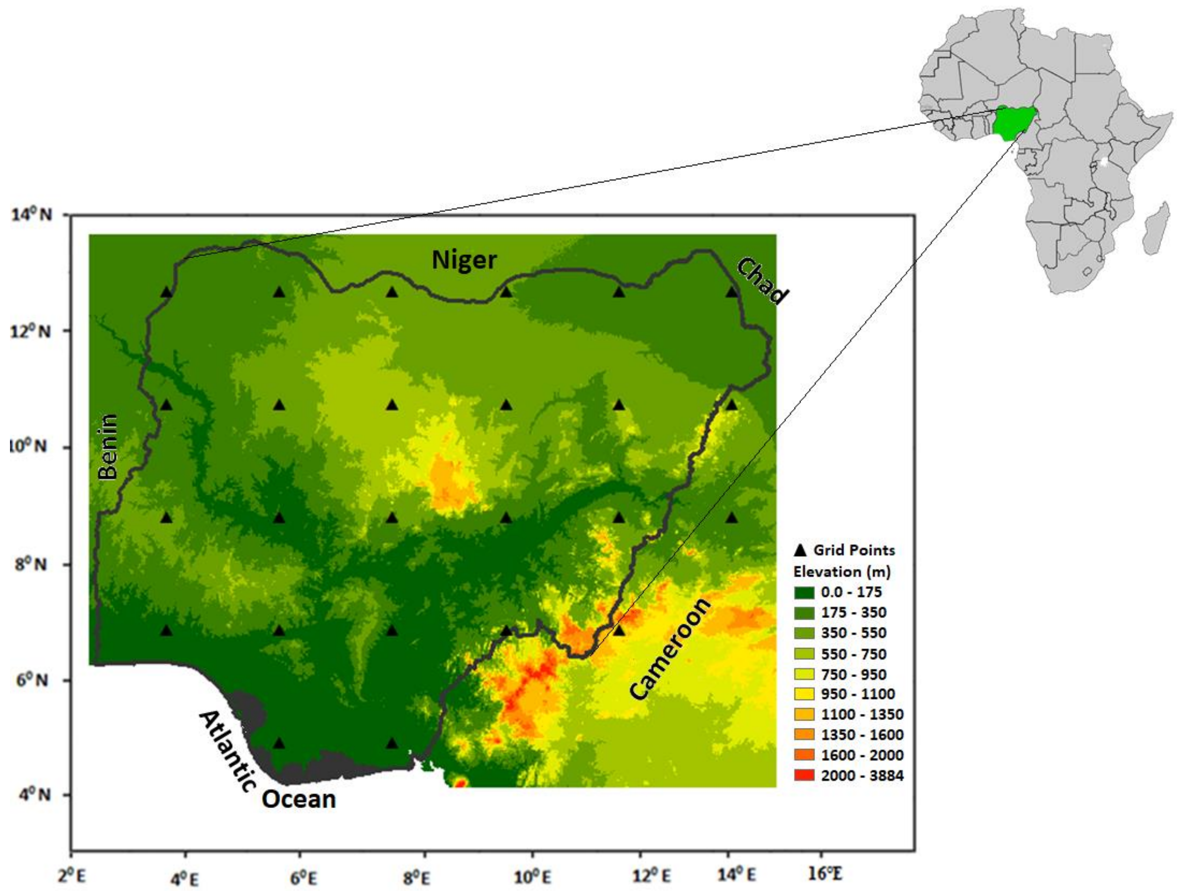

Figure 1. Map of Nigeria showing the elevations, bordering countries and grid points considered in the study.

2.2. Gauged based gridded precipitation and temperature data

Like in many developing nations, there is difficulty in accessing reliable climate data in Nigeria. Firstly, due to the sparse distribution of gauges across the country; only 87 operating rain gauges are available as against the recommended 1057 and gauge density of 874 km2 by World Meteorological Organization (WMO, 1965) for appropriately measuring precipitation (Ngene et al., 2015). Secondly, there is the incompleteness of data for some of the stations or some are not available at the long-term. Therefore, this study uses a 0.5^{o}x 0.5^{o} grid resolution GPCC V6 monthly full reanalysis data product of the Deutscher Wetterdienst (Becker et al., 2013) and monthly maximum and minimum temperature CRU TS v. 3.23 of the East Anglia University (Harris et al., 2014) for the period 1984 - 2014. Due to the lack of sufficient data, the GPCC precipitation and the CRU temperature products have been found to be suitable for climate studies over the African continent including in Nigeria (Diallo et al., 2018; Shiru et al., 2020b; Shiru et al., 2019b; Tirivarombo et al., 2018).

The monthly precipitation data of the GPCC are produced based on over 85,000 rain gauge stations from about 190 countries. A smart interpolation technique which considers the systematic relationship between elevation and station observations which enhances the estimation accuracies is used in the production of the GPCC (Funk et al., 2007).

The CRU employs measurements from about 4,000 monitoring stations across the globe. The product undergoes an extensive two stages, manual and semi-automatic quality control measures; the first being to ensure consistency, and the second involving removal of stations or months with large errors. The production of the world's land-based gridded temperature data by the CRU has been of great significance to the international community especially in climate research as it has been widely used in the assessment of the changes in temperature across the globe.

2.3 Global Climate Models

This study uses the historical precipitation and temperature of the newly released CMIP6 GCMs. In the CMIP6 phase, the representative concentration pathways (RCPs) scenarios' RCP2.6, RCP4.5, RCP6.0 and RCP8.5 of the CMIP5 have been updated to Shared Socio-economic Pathways (SSPs): SSP1-2.6, SSP2-4.5, SSP4-6.0, and SSP5-8.5 respectively, each of which also considers 2100 radiative forcing levels. The climate change research community established the SSPs for facilitation of the integrated analysis of the future climate vulnerabilities, impacts, adaptation and mitigation (Riahi et al., 2017). According to (Hausfather, 2018), the SSPs involves five possibilities which are: (1) a situation of sustainability-focused growth and equality (SSP1); (2) a situation where the trends follow their historical patterns broadly (SSP2); (3) a fragmented world of "resurgent nationalism" (SSP3); (4) an ever increasing inequality world; and (5) a situation of rapid and unconstrained growth in energy use and economic output (SSP5). The CMIP6 through improved emissions, land use scenarios, improved physical processes and model parameterization is targeted to robustly unfold the future conditions of the climate (Eyring et al., 2016; O'Neill et al., 2016). In this study, 13 sets of historical GCMs each for precipitation and maximum and minimum temperature were chosen from the CMIP6 database for the period

1984–2014. The period 1984–2014 was considered since the CMIP6 GCMs have are up to 2014 and to have a 30 years baseline period as was considered for CMIP5. The GCMs were chosen based on the availability of at least one SSP for the future period, common GCMs among precipitation and temperature variables, and their availability for the study area. There are several ensemble members of the CMIP6 including r1i1l1f1, r2i1l1f1, r3i1l1f1 representing the realization, initialization and the models' physics. The first ensemble members; r1i1l1f1, of the GCMs' were considered in order to have an unbiased comparison of all of them. Information about the GCMs of the CMIP6 models chosen for this study is provided in Table 1.

Table 1. Basic information of the GCMs of the CMIP6 used in this study.

No	Institution - Country	CMIP6 Model Name	Resolution (lon. by lat. in degrees)
1	Australian Community Climate and Earth	ACCESS-CM2	1.9°×1.3°
2	System Simulator - Australia	ACCESS-ESM1-5	1.9°×1.2°
3	Alfred Wegener Institut - Germany	AWI-CM-1-1-MR	1.1°× 1.1°
4	Max-Planck-Institut für Meteorologie - Germany	MPI-ESM1-2-LR	1.9°× 1.9°
5	Canadian Centre for Climate Modelling and Analysis - Canada	CanESM5	2.8°×2.8°
6	Centro Euro Mediterraneo sui Cambiamenti Climatici - Italy	CMCC-CM2-SR5	1.25° × 1.0°
7	Marchuk Institute of Numerical Mathematics -	INM-CM4-8	2°×1.5°
8	Russia	INM-CM5-0	2°×1.5°
9	Institut Pierre-Simon Laplace - France	IPSL-CM6A-LR	2.5°× 1.3°
10	The University of Tokyo, National Institute for Environmental Studies, and Japan Agency for Marine-Earth Science and Technology - Japan	MIROC6	1.4°× 1.4°
11	Meteorological Research Institute - Japan	MRI-ESM2-0	1.1°× 1.1°
12	Beijing Climate Center - China	BCC-CSM2-MR	1.1°× 1.1°
13	Nanjing University of Information Science and Technology - China	NESM3	1.9°×1.9°

3. Methodology

The methods applied in this study are presented in this section. Before the assessments, the GPCC precipitation, the CRU maximum and minimum temperature and all GCMs were re-gridded to 2° × 2° resolution using bilinear interpolation to have a uniform resolution. The 2° × 2° resolution was chosen as it is approximately equal to the average spatial resolution of most of the GCMs (Ahmed et al., 2019b). Bilinear interpolation is often conducted for smoothly transforming spatially coarse GCM data into finer data through GCM data interpolation from the four nearest neighboring grid points (Almazroui et al., 2020b; Penalba and Rivera, 2016). The methods applied in this study are discussed as follows.

3.1 Statistical Indices

The ability of the different GCMs in reproducing the properties of the observed at the 25 grid points of the study area were assessed using five statistical indices: NRMSE, Pbias, NSE, R^2 and VE. The expressions used to describe statistical metrics used here: x_{pred}; i and x_{obs}; i are the i-th gridded and observed data, which is the number of observations. Details about the statistical metrics used in this study are as follows.

The magnitude of the errors in predictions for various times is summarized by the NRMSE, making it a good measure of accuracy (Willmott, 1982). The closer the NRMSE value is to zero, the more accurate the model is (Chen and Liu, 2012; Johnston, 2004). It is a normalized statistic determining the relative magnitude of the residual variance to the variance of the measured data. Smaller NRMSE values (preferably zero) indicate better performance of the model (Raju et al., 2017). It is defined as follows.

$$NRMSE = \frac{\left[\frac{1}{n}\sum_{i=1}^{n}\left(x_{pred,i}-x_{obs,i}\right)^2\right]^{1/2}}{\frac{1}{n}\sum_{i=1}^{n}\left(x_{pred,i}\right)} \quad (1)$$

The models data tendency to under or over-estimate the observed data is measured by the Pbias. A model performance is better when the Pbias values are closer to zero. A negative Pbias value is an indication of overestimation while a positive one indicates underestimation (Gupta et al., 1999). The evaluation of Pbias is conducted as follows.

$$Pbias = 100 \times \left[\frac{\sum_{i=1}^{n}\left(x_{pred,i}-x_{obs,i}\right)}{\sum_{i=1}^{n}x_{pred,i}}\right] \quad (2)$$

The quantitative statistic of (Nash and Sutcliffe, 1970) is defined as one minus the sum of the absolute squared differences between the predicted and the observed values normalized by the variance of the observed value during the period under investigation. With 1 being the optimal value, the NSE can have values between -∞ and 1.0. NSE values from 0.0 and 1.0 are considered acceptable levels of performance, whereas values < 0.0 are indicative of unacceptable model performance in which the mean observed value is a better predictor than the simulated value (Moriasi et al., 2007). NSE can be computed as follows.

$$NSE = 1 - \frac{\sum_{i=1}^{n}\left(x_{pred,i} - x_{obs,i}\right)^2}{\sum_{i=1}^{n}\left(x_{obs,i} - \overline{x_{obs}}\right)^2} \qquad (3)$$

The R^2 can be defined as the square of the Pearson's product moment correlation coefficient (i.e. $R^2 = r^2$) describing the proportion of the total variance in the observed data which is explainable by the model (Legates and McCabe Jr, 1999). R^2 values can range between 0.0 and 1.0, in which the higher value indicates a better agreement. Computation of R^2 is as follows.

$$R^2 = \frac{\sum_{i=1}^{N}\left(x_{obs,i} - \overline{x_{obs}}\right)\left(x_{\mathrm{Pred},i} - \overline{x_{\mathrm{Pred}}}\right)}{\sqrt{\sum_{i=1}^{N}\left(x_{\mathrm{Pred},i} - \overline{x_{\mathrm{Pred}}}\right)^2 \sum_{i=1}^{N}\left(x_{obs,i} - \overline{x_{obs}}\right)^2}} \qquad (4)$$

The VE measures the ratio between GCM and GPCC precipitation volumes over a period, where a VE value of 1 indicates a perfect estimation. It is can be calculated using the following equation.

$$VE = 1 - \frac{\sum_{i=1}^{n}\left(x_{pred,i} - x_{obs,i}\right)}{\sum_{i=1}^{n} x_{obs,i}} \qquad (5)$$

3.2 Compromise Programming

CP (Zeleny, 1973) is an approach applicable in the measurement of the combined effect of several statistical indices. CP was employed in this study for ranking of GCMs based on five statistical performance measures described above, NRMSE, Pbias, NSE, R^2 and VE. The statistical indices values were used for the estimation of the distance measure (*Lp*) metric of CP. L_p metric is given as:

$$L_p = \left[\sum_{j=1}^{1} |f_j^* - f_j|^p\right]^{1/p} \qquad (6)$$

where f_j is the value of the statistical performance measure j, f_j^* is the ideal value of the statistical performance measure j, and p is a parameter which is equal to 1. For a statistical performance measure, the ideal value is that corresponding to a perfect match between relevant observations and the simulations produced by the model. The value of the L_p metric is always positive, and the lower the value, the higher the performance of the model; therefore the smallest values of L_p is preferred.

In addition, the abilities of the GCMs to replicate the climate properties of the study area were also assessed using spatial comparisons, PDF, TD, and the plots of the annual and monthly averages of the observed and the GCMs.

4. Results

4.1 Ranking of GCMs using CP

4.1.1 Ranking of GCMs for precipitation

The performance metrics for precipitation calculated for all GCMs and the ranking of GCMs derived using CP is shown in Table 2. Though the ideal values vary from GCM to GCM, the overall ranking indicates that a GCM which may have its value as the most ideal for more metrics may not necessarily rank best. For example, ACC.ESM1.5 has two of its metrics as the ideal values but ranked 4th in terms of the overall ranking of the GCMs. For precipitation, the four highest ranked GCMs are IPSL.CM6A-LR, NESM3, CMCC.CM2-SR5, and ACC.ESM1.5 in that order. The least performing GCM for precipitation is INM.CM4.8.

Table 2. Performance metrics and ranking of precipitation GCMs using CP method.

GCMs	Performance metrics					Difference in metrics and ideal values					Sum	Rank
	NRMSE	Pbias	R^2	NSE	VE	NRMSE	Pbias	R^2	NSE	VE		
ACCESS-CM2	68.2	-30.7	0.83	0.53	0.61	30.2	30.5	0.06	0.33	0.18	61.27	10
ACCESS-ESM1-5	49.9	0.2	0.77	0.75	0.73	11.9	0	0.12	0.11	0.06	12.19	4
AWI-CM-1-1-MR	50.9	-27.4	0.88	0.74	0.67	12.9	27.2	0.01	0.12	0.12	40.35	8
BCC-CSM2-MR	61.9	15.7	0.69	0.62	0.69	23.9	15.5	0.2	0.24	0.1	39.94	7
CanESM5	49.9	17.7	0.81	0.75	0.71	11.9	17.5	0.08	0.11	0.08	29.67	6
CMCC.CM2-SR5	41.5	7.1	0.87	0.83	0.79	3.5	6.9	0.02	0.03	0	10.45	3
INM-CM4-8	99.8	-43.8	0.88	0	0.51	61.8	43.6	0.01	0.86	0.28	106.55	13
INM-CM5-0	89.5	-29.6	0.84	0.2	0.58	51.5	29.4	0.05	0.66	0.21	81.82	11
IPSL-CM6A-LR	38	2	0.86	0.86	0.79	0	1.8	0.03	0	0	1.83	1
MIROC6	43.6	-11.5	0.83	0.81	0.76	5.6	11.3	0.06	0.05	0.03	17.04	5
MPI-ESM-1-2-LR	71	-49	0.89	0.49	0.49	33	48.8	0	0.37	0.3	82.47	12
MRI-ESM2-0	65.9	-16.4	0.67	0.56	0.6	27.9	16.2	0.22	0.3	0.19	44.81	9
NESM3	39.2	-6.1	0.86	0.85	0.71	1.2	5.9	0.03	0.01	0.08	7.22	2
Ideal Values	38	0.2	0.89	0.86	0.79							

4.1.2 Ranking of GCMs for maximum temperature

The performance metrics for maximum temperature calculated for all GCMs and the ranking of GCMs derived using CP is presented in Table 3. The highest ranking GCMs are INM-CM4-8, BCC-CSM2-MR, MRI-ESM2-0, and ACCESS-ESM1-5 in respective order. The least ranking GCM for the maximum temperature using CP method was CMCC.CM2-SR5.

Table 3. Performance metrics and ranking of maximum temperature GCMs using CP method.

GCMs	Performance metrics					Difference in metrics and ideal values					Sum	Rank
	NRMSE	Pbias	R^2	NSE	VE	NRMSE	Pbias	R^2	NSE	VE		
ACCESS-CM2	106.7	2	0.42	-0.14	0.96	47.9	2	0.32	0.51	0.01	50.74	9
ACCESS-ESM1-5	70.2	-1.3	0.65	0.51	0.97	11.4	1.3	0.09	0.14	0	12.93	4
AWI-CM-1-1-MR	76.7	4.7	0.74	0.41	0.95	17.9	4.7	0	0.24	0.02	22.86	6
BCC-CSM2-MR	63.5	0.7	0.73	0.6	0.97	4.7	0.7	0.01	0.05	0	5.46	2
CanESM5	86.7	0	0.36	0.25	0.95	27.9	0	0.38	0.4	0.02	28.7	7
CMCC.CM2-SR5	362.6	-22.4	0.31	-12.18	0.78	303.8	22.4	0.43	11.53	0.19	338.35	13
INM-CM4-8	58.8	-2	0.74	0.65	0.97	0	2	0	0	0	2	1
INM-CM5-0	74.3	-2.6	0.68	0.45	0.96	15.5	2.6	0.06	0.2	0.01	18.37	5
IPSL-CM6A-LR	231.5	-11	0.7	-4.37	0.88	172.7	11	0.04	3.72	0.09	187.55	12
MIROC6	109.7	7.9	0.62	-0.21	0.89	50.9	7.9	0.12	0.44	0.08	59.44	10
MPI-ESM-1-2-LR	84.8	-4.4	0.58	0.28	0.95	26	4.4	0.16	0.37	0.02	30.95	8
MRI-ESM2-0	64.2	-0.1	0.6	0.59	0.97	5.4	0.1	0.14	0.06	0	5.7	3
NESM3	207.9	-21.7	0.26	-3.33	0.78	149.1	21.7	0.48	2.68	0.19	174.15	11
Ideal Values	58.8	0	0.74	0.65	0.97					0.01	50.74	

4.1.3 Ranking of GCM for minimum temperature

The performance metrics for maximum temperature calculated for all GCMs and the ranking of GCMs derived using CP is presented in Table 4. The highest ranking GCMs are AWI-CM-1-1-MR, IPSL-CM6A-LR, INM-CM5-0, and CanESM5 in respective order. The least ranking GCM for the minimum temperature similar to that of the maximum temperature was also CMCC.CM2-SR5.

Table 4. Performance metrics and ranking of minimum temperature GCMs using CP method.

MODELS	Performance metrics					Difference in metrics and ideal values					Sum	Rank
	NRMSE	Pbias	R^2	NSE	VE	NRMSE	Pbias	R^2	NSE	VE		
ACCESS-CM2	85.3	7.7	0.73	0.27	0.89	41.4	7.4	0.15	0.54	0.06	49.55	9
ACCESS-ESM1-5	69.1	6	0.76	0.52	0.92	25.2	5.7	0.12	0.29	0.03	31.34	7
AWI-CM-1-1-MR	43.9	0.3	0.87	0.81	0.95	0	0	0.01	0	0	0.01	1
BCC-CSM2-MR	74.7	5.5	0.73	0.44	0.93	30.8	5.2	0.15	0.37	0.02	36.54	8
CanESM5	63.6	1.4	0.69	0.59	0.89	19.7	1.1	0.19	0.22	0.06	21.27	4
CMCC.CM2-SR5	345.4	21.8	0.71	-10.96	0.75	301.5	21.5	0.17	10.15	0.2	333.52	13
INM-CM4-8	62	-4	0.75	0.61	0.91	18.1	3.7	0.13	0.2	0.04	22.17	5
INM-CM5-0	55.5	-1.9	0.76	0.69	0.93	11.6	1.6	0.12	0.12	0.02	13.46	3
IPSL-CM6A-LR	54	1.2	0.72	0.71	0.94	10.1	0.9	0.16	0.1	0.01	11.27	2
MIROC6	92.4	9	0.82	0.14	0.9	48.5	8.7	0.06	0.67	0.05	57.98	10
MPI-ESM-1-2-LR	61.5	6	0.88	0.62	0.92	17.6	5.7	0	0.19	0.03	23.52	6
MRI-ESM2-0	116.8	10.8	0.8	-0.37	0.87	72.9	10.5	0.08	0.44	0.08	84	11
NESM3	126.7	15.2	0.82	-0.61	0.83	82.8	14.9	0.06	0.2	0.12	98.08	12
Ideal Values	43.9	0.3	0.88	0.81	0.95							

4.2 Spatial analysis

4.2.1 Spatial comparison of GCMs with GPCC precipitation

The ability of the different GCMs to spatially replicate the average annual GPCC precipitation over the period 1984 - 2014 is presented in Figure 2. The performances of the GCMs vary in their abilities to reproduce the GPCC precipitation though almost all GCMs show similarities in some regions such as the lower precipitation in the north eastern arid region of the country. Four GCMs namely, AWI-CM-1-1-MR, CanESM5, BCC-CSM2-MR, and CMCC.CM2-SR5 overestimated the precipitation at the south west of the country. Precipitation was mostly underestimated by INM-CM4-8, INM-CM5-0, and MPI-ESM-1-2-LR. The GCMs ranked high by the CP method were seen to have better abilities in spatially replicating the historical precipitation in Nigeria.

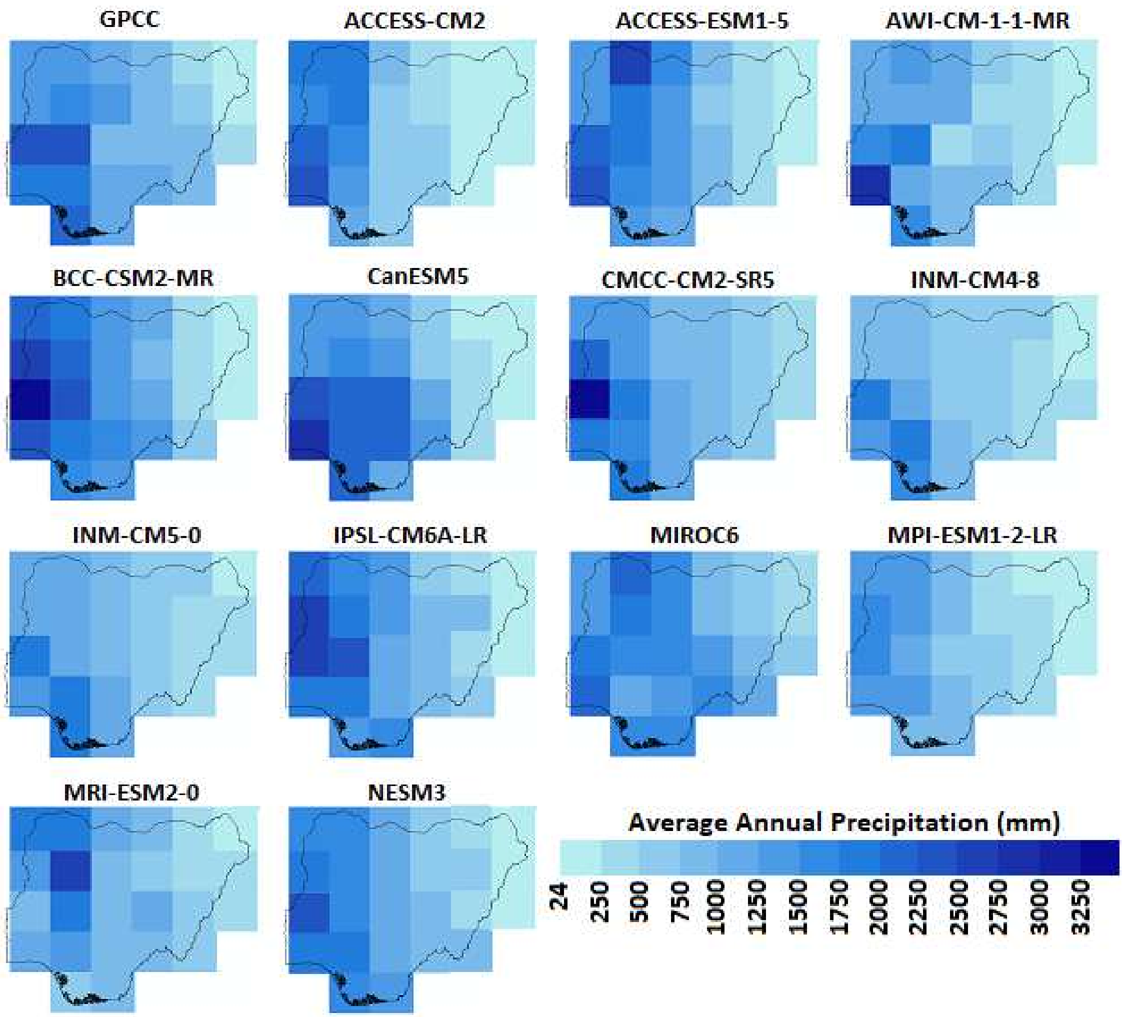

Figure 2 Spatial comparisons of historical GCMs with GPCC average annual precipitation over Nigeria for the period 1984 – 2014.

4.2.2 Spatial Comparison of GCMs with CRU Maximum Temperature

The ability of the different GCMs to spatially replicate the CRU mean annual maximum temperature is presented in Figure 3. MIROC6 showed a significant overestimation of the temperature at the north east of the country. The spatial assessment result is in agreement with the result of the CP for maximum temperature which ranked NESM3, IPSL-CM6A-LR, and CMCC-CM2-SR5 as the lowest. These GCMs underestimated the maximum temperature in the study area relative to the CRU. The highest ranking GCMs INM-CM4-8, BCC-CSM2-MR, MRI-ESM2-0 and ACCESS-ESM1-5 showed close spatial relationship with the CRU maximum temperature.

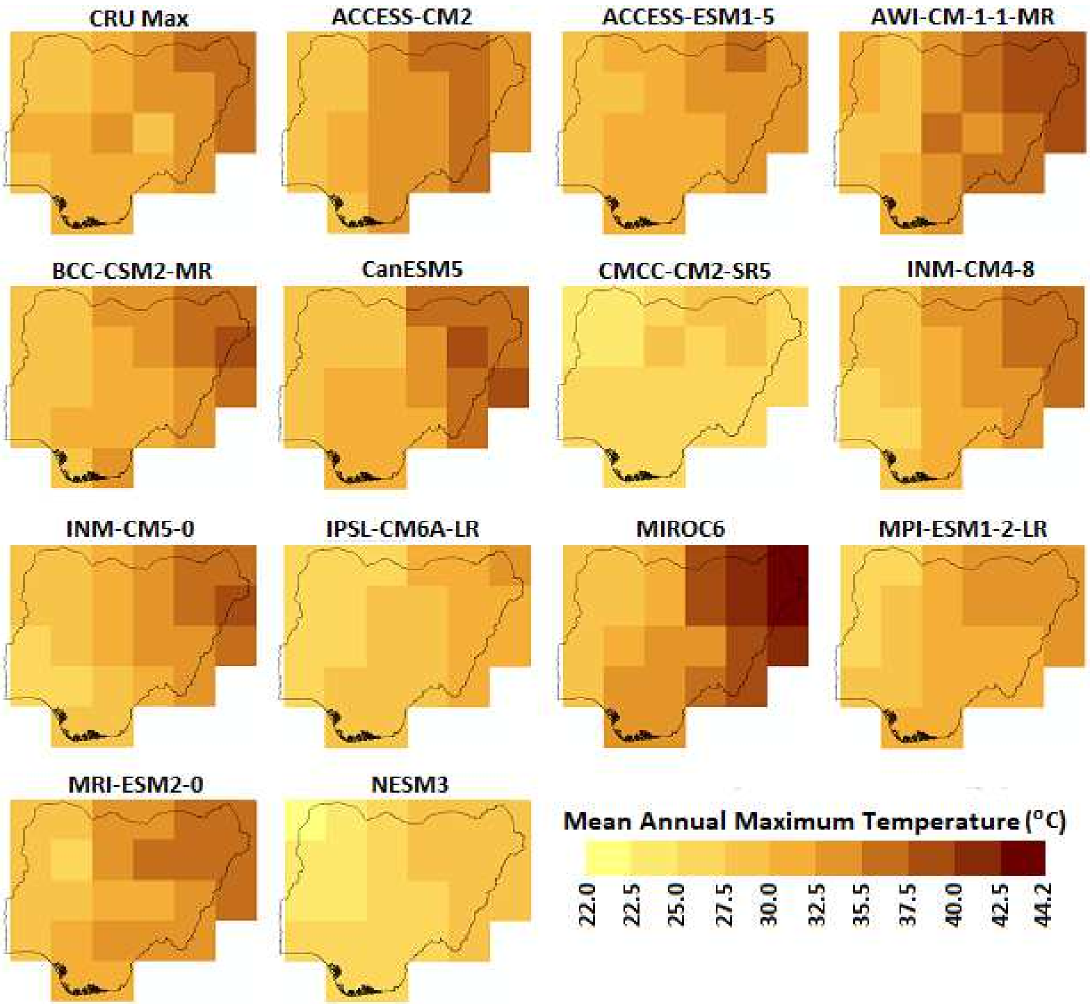

Figure 3 Spatial comparisons of historical GCMs with CRU mean annual maximum temperature over Nigeria for the period 1984 – 2014.

4.2.3 Spatial Comparison of GCMs with CRU Minimum Temperature

The ability of the different GCMs to spatially replicate the CRU mean annual minimum temperature is presented in Figure 4. Figure show all the GCMs overestimated the minimum temperature relative to the CRU minimum temperature particularly MRI-ESM2-0, NESM3 and CMCC-CM2-SR5 which are the lowest ranking ones. The highest ranking GCMs from the CP showed better skills in replicating the minimum CRU temperature over the country.

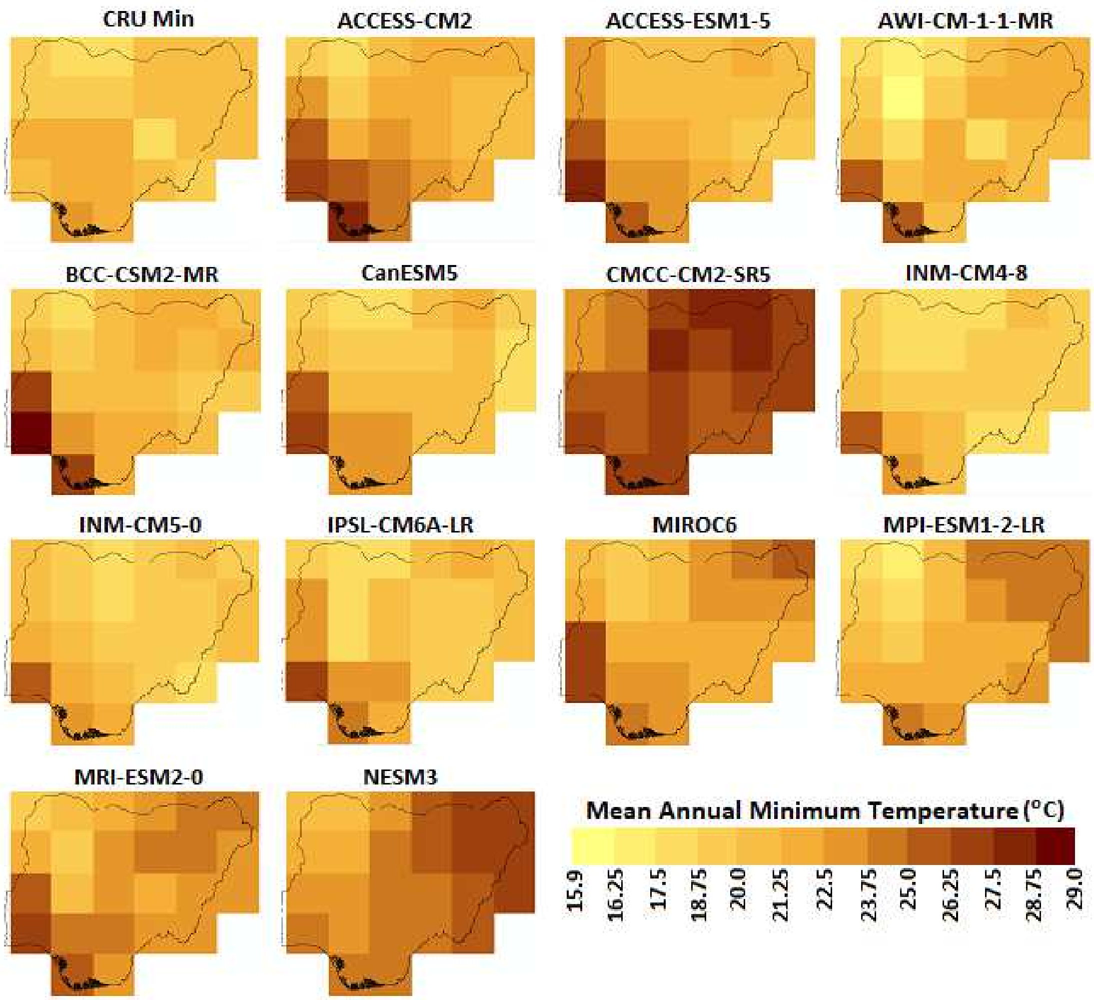

Figure 4 Spatial comparisons of historical GCMs with CRU mean annual minimum temperature over Nigeria for the period 1984 – 2014.

4.3 Comparison using probability density function

The PDFs of the mean monthly precipitation, maximum temperature, and minimum temperature compared with the observed GPCC and CRU for the period 1984 – 2014 in Nigeria are presented in Figure 5a, 5b, and 5c, respectively. Figures show that most of the GCMs were able to replicate the precipitation properties of the GPCC especially from the tailing. However, the distribution of precipitation relative to the GPCC varies more in the GCMs INM-CM4-8, INM-CM5-0, and MPI-ESM1-2-LR which showed the least rankings in the CP and spatial underestimation of the precipitation. For maximum temperature, the underestimations by CMCCC-CM2-SR5, IPSL-

CM6A-LR, and NESM3 are visible in the PDF plots while the overestimations by MIROC6 and AWI-CM-1-1-MR are seen. PDF distributions show that most of the maximum temperature distributions are around 30°C. For minimum temperature; the PDFs of the GCMs compared to the CRU show an overestimation by all GCMs which is supported by the spatial assessment.

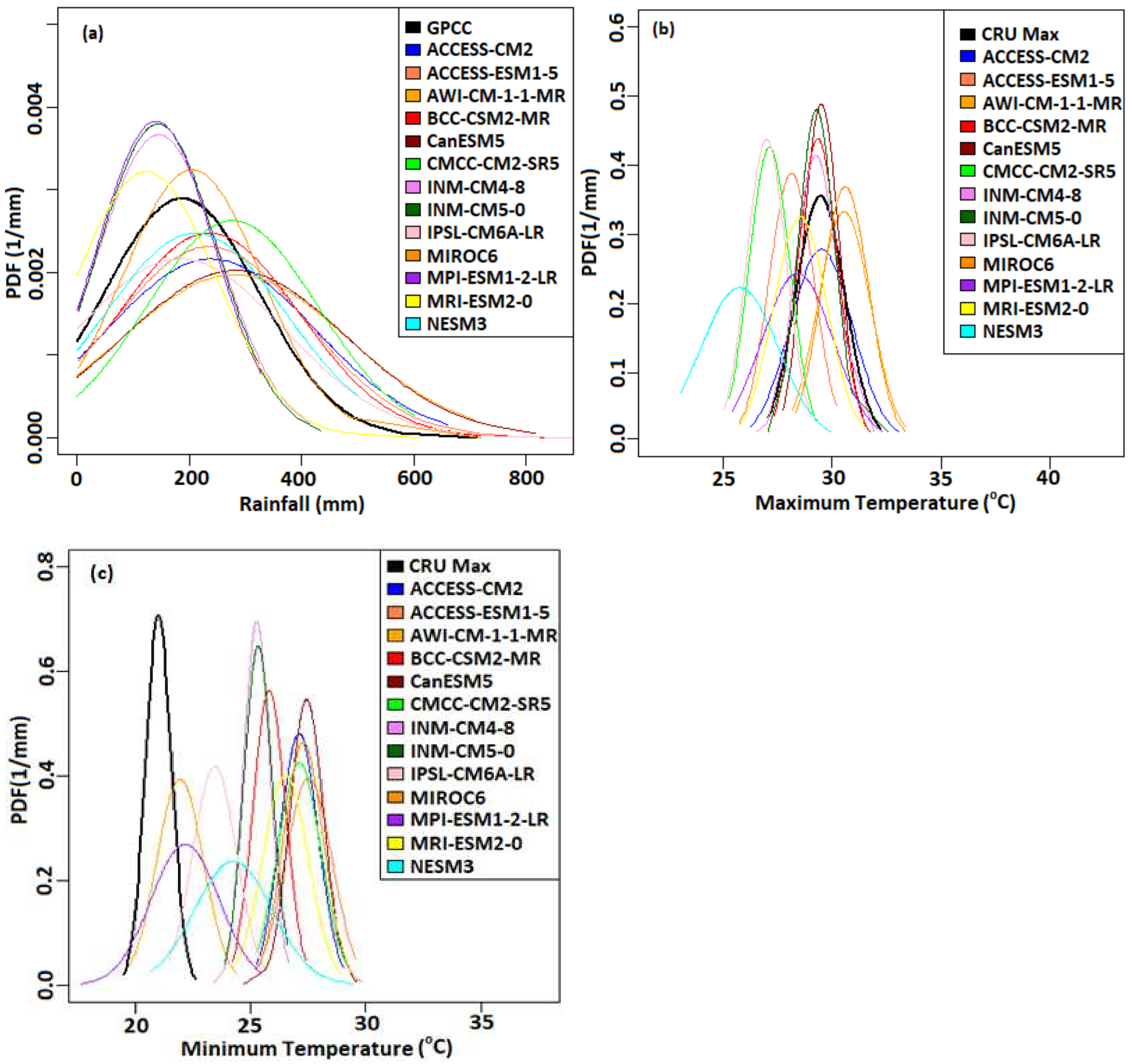

Figure 5 PDFs comparing mean monthly observed (a) GPCC precipitation, (b) CRU maximum temperature, and (c) CRU minimum temperature to the GCMs.

4.4 Performance assessment using Taylor diagram

TD (Taylor, 2001) has the ability to give a good statistical summary of correlation, standard deviation and root-mean-square (RMS) between the modelled and the observed data. Figure 6(a), 6(b) and 6(c) show the performances of the precipitation, maximum temperature and minimum temperature GCMs respectively relative to their observed data using TD. Though the standard deviations are all different, the correlation between the modelled and observed ranges from 0.8 – 0.91. The highest ranking GCMs were seen to have higher correlations.

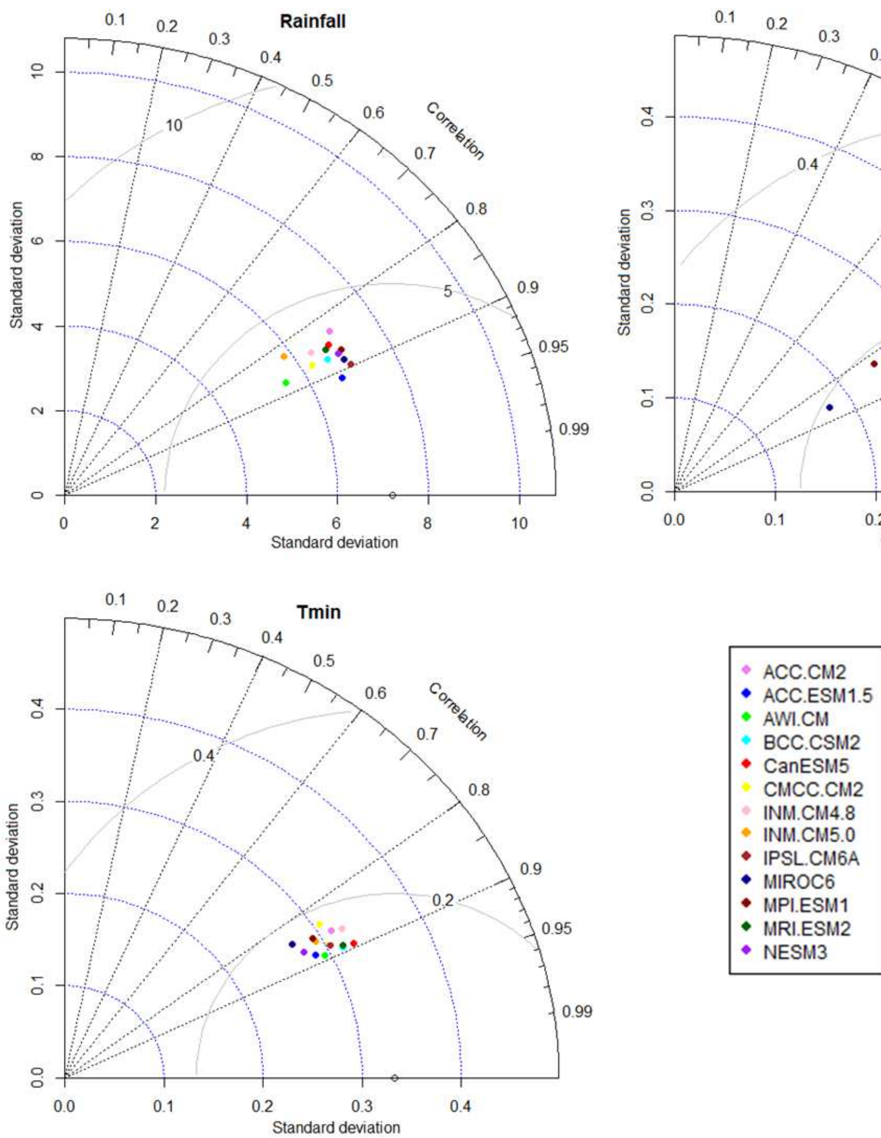

Figure 6 Taylor diagram showing the correlation of (a) GCM precipitation with GPCC, (b) GCM maximum temperature with maximum CRU, and (c) GCM minimum temperature with minimum CRU.

4.5 Comparison of the mean monthly precipitation and temperature of GCMs with the observed

The mean monthly precipitation, maximum temperature, and minimum temperature for the GCMs compared to the observed for 1984-2014 are presented in Figures 7(a), 7(b), and 7(c), respectively. For precipitation, it can be seen that most of the models have good performance during the dry seasons from November to March when there are little or no variability in precipitations. There is high variability in the estimated precipitation by the GCMs relative to the GPCC during the wet season (April – October) in the country. Though with a little over/under estimation of precipitation during the peak of wet season in August, the highest performing GCMs, IPSL-CM6A-LR, NESM3, CMCC-CM2-SR5, and ACCESS-ESM1-5 showed higher capability of replicating the mean monthly for the wet season. There were however significant underestimation by ACCESS-CM2, INM-CM5-0, INM-CM4-8, and MPI-.ESM1-2-LR.

For maximum temperature, the least ranking GCMs CMCC-CM2-SR5, NESM3, and IPSL-CM6A-LR showed underestimation of the maximum temperature. The highest ranking GCMs INM-CM4-8, BCC-CSM2-MR, MRI-ESM2-0 and ACCESS-ESM1-5 as calculated from the CP show better similarity with the CRU. Over estimation was most significant by MIROC6 and AWI-CM-1-1-MR.

For minimum temperature, significant overestimation was observed for NESM3 and CMCC-CM2-SR5. Other GCMs also overestimated minimum temperatures during April and October. There was also some few under estimation of the minimum temperature by some GCMs during between the months of October and April. The highest ranking GCMs AWI-CM-1-1-MR, IPSL-CM6A-LR, INM-CM5-0, and CanESM5 show more closeness to the CRU.

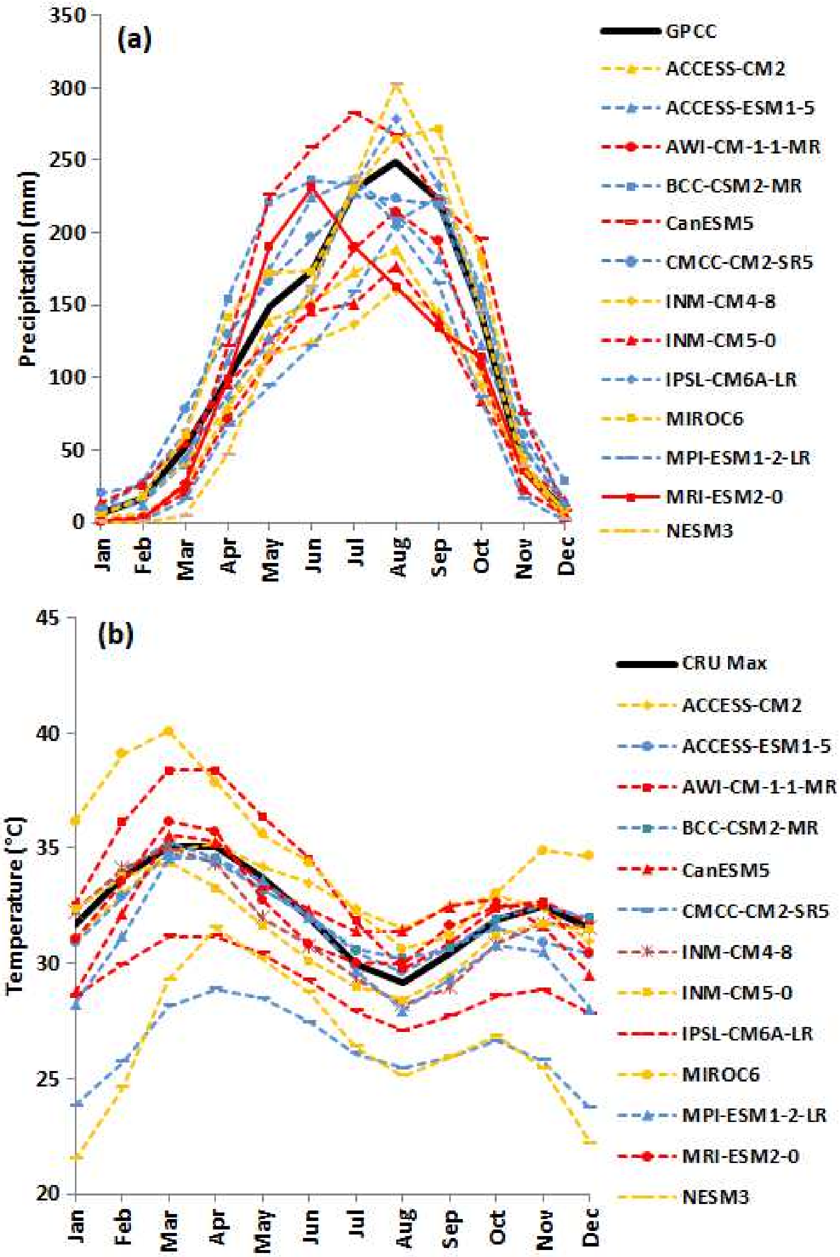
(a)
Precipitation (mm)
350
300
250
200
150
100
50
0
Jan
Feb
Mar
Apr
May
Jun
Jul
Aug
Sep
Oct
Nov
Dec
GPCC
ACCESS-CM2
ACCESS-ESM1-5
AWI-CM-1-1-MR
BCC-CSM2-MR
CanESM5
CMCC-CM2-SR5
INM-CM4-8
INM-CM5-0
IPSL-CM6A-LR
MIROC6
MPI-ESM1-2-LR
MRI-ESM2-0
NESM3
(b)
Temperature (°C)
45
40
35
30
25
20
Jan
Feb
Mar
Apr
May
Jun
Jul
Aug
Sep
Oct
Nov
Dec
CRU Max
ACCESS-CM2
ACCESS-ESM1-5
AWI-CM-1-1-MR
BCC-CSM2-MR
CanESM5
CMCC-CM2-SR5
INM-CM4-8
INM-CM5-0
IPSL-CM6A-LR
MIROC6
MPI-ESM1-2-LR
MRI-ESM2-0
NESM3

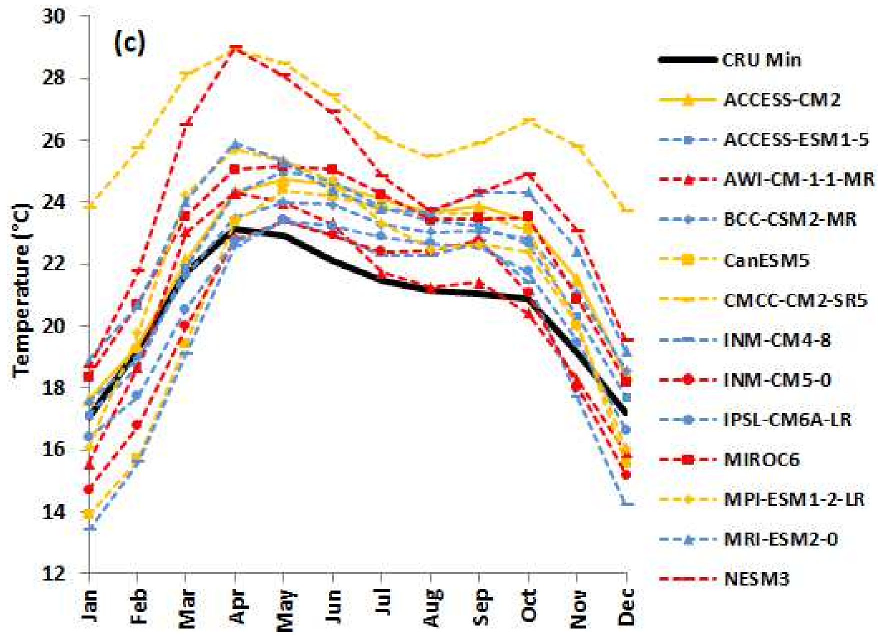

Figure 7 Comparison of mean monthly (a) GCM precipitation and GPCC, (b) GCM maximum temperature and CRU maximum temperature, (c) GCM minimum temperature and CRU minimum temperature.

4.7 Selection of multi model ensemble for climate change projection

The scores and final rankings of the different GCMs in replicating the observed precipitation and maximum and minimum temperature derived using CP are shown in Table 5. For precipitation, the highest ranking GCMs are IPSL-CM6A-LR, NESM3, CMCC-CM2-SR5, and ACCESS-ESM1-5. INM-CM4-8, BCC-CSM2-MR, MRI-ESM2-0, and ACCESS-ESM1-5 ranked the highest for maximum temperature while AWI-CM-1-1-MR, IPSL-CM6A-LR, INM-CM5-0, and CanESM5 ranked the highest for the minimum temperature. The lowest ranking GCMs for precipitation are INM-CM4-8, MPI-.ESM1-2-LR, INM-CM5-0, and ACCESS-CM2; the lowest for maximum temperature are CMCC-CM2-SR5, IPSL-CM6A-LR, NESM3, and MIROC6, while CMCC-CM2-SR5, NESM3, MRI-ESM2-0, and MIROC6 ranked lowest for the minimum temperature.

Table 5. Final ranking of GCMs using CP method (bold GCMs are the most suitable for the study area while GCMs in italic are the least suitable).

Precipitation			Max Temp			Min Temp		
GCM	Score	Rank	GCM	Score	Rank	GCM	Score	Rank
IPSL-CM6A-LR	1.83	1	**INM-CM4-8**	2	1	**AWI-CM-1-1-MR**	0.01	1
NESM3	7.22	2	**BCC-CSM2-MR**	5.46	2	**IPSL-CM6A-LR**	11.27	2
CMCC-CM2-SR5	10.45	3	**MRI-ESM-2-0**	5.7	3	**INM-CM5-0**	13.46	3
ACCESS-ESM1-5	12.19	4	**ACCESS-ESM1-5**	12.93	4	**CanESM5**	21.27	4
MIROC6	17.04	5	INM-CM5-0	18.37	5	INM-CM4-8	22.17	5

CanESM5	29.67	6	AWI-CM-1-1-MR	22.86	6	MPI-.ESM1-2-LR	23.52	6
BCC-CSM2-MR	39.94	7	CanESM5	28.7	7	ACCESS-ESM1-5	31.34	7
AWI-CM-1-1-MR	40.35	8	MPI-.ESM1-2-LR	30.95	8	BCC-CSM2-MR	36.54	8
MRI-ESM2-0	44.81	9	ACCESS-CM2	50.74	9	ACCESS-CM2	49.55	9
ACCESS-CM2	61.27	10	*MIROC6*	59.44	10	*MIROC6*	57.98	10
INM-CM5-0	81.82	11	*NESM3*	174.15	11	*MRI-ESM2-0*	84	11
MPI-.ESM1-2-LR	82.47	12	*IPSL-CM6A-LR*	187.55	12	*NESM3*	98.08	12
INM-CM4-8	106.55	13	*CMCC-CM2-SR5*	338.35	13	*CMCC-CM2-SR5*	333.52	13

5. Discussion

The trends of increasing temperature and changes in precipitation are expected to intensify under different climate change scenarios of the previous assessment reports (AR) (Homsi et al., 2020; Onyutha et al., 2016; Sa'adi et al., 2019). The expected changes are also projected to increase incidences of disasters and its risks. While understanding these expected changes through climate projection is imperative for the development of adaptation and mitigation measures against climate change, the choice of GCM or the generation of MME is even more crucial for a region. This is due to the different uncertainties associated with them, which may result from GCM initialization and parameterization (Tebaldi et al., 2005) and future GHG emission and aerosols content scenarios (Hawkins and Sutton, 2009) giving them characteristically varying spatial performances across the globe (Chen et al., 2017).

Though the newly released CMIP6 has been used for the projection of climate over the globe including Africa (Almazroui et al., 2020a; Zhai et al., 2020), no study has yet specifically applied it in Nigeria as at the time of this study. Therefore, the projection of climate using CMIP6 is crucial for the country which majority of its rural populace depend on rain-fed agricultural, which constitutes 20% of the gross domestic products (GDP). In addition, the country has one of the highest rates of population growth, which would need more water resources, a resource grossly affected by climate. Water resources in the country has been reported to be declining (MacDonald et al., 2005) and a recent study projected groundwater levels will drop to as much as 12 m in some parts of the country in the future (Shiru et al., 2020a). This emphasizes the need to conduct climate projection using reliable GCMs.

Among studies that have evaluated the CMIP6 performances on the African continent, (Babaousmail et al., 2021) considering fifteen precipitation GCMs and using a combination of statistical metrics, empirical cumulative distribution function, Taylor skill score and Taylor diagram, found that the CMIP6 GCMs were satisfactorily able to reproduce mean annual climatology of dry/wet months in the northern of the continent. The study found EC-Earth3-Veg, UKESM1-0-LL, GFDL-CM4, NorESM2-LM, IPSLCM6A-LR, and GFDL-ESM4 as the best performing models. Similar to their study, this present study also found the IPSLCM6A-LR to have a good performance for Nigeria. The study found that there was mostly underestimation of the precipitation by the GCMs during the wet seasons, a finding similar to that of ours.

In the eastern part of East Africa, covering Kenya, Rwanda, Tanzania, Uganda, and Burundi, thirteen CMIP6 temperature GCMs were used in evaluating mean surface temperature (Ayugi et al., 2021b) by employing statistical metrics, mean state, and trends. The study found that most of the GCMs overestimated the mean annual temperature with few underestimating it. FGOALSg3, HadGEM-GC31-LL, MPI-ESM2-LR, CNRM-CM6-1, and IPSL-CM6A-LR were the models found to be the best performing in the study. Since this study and ours mostly considered different GCMs and different temperature parameters; mean temperature in the former and maximum and minimum temperature in the later, in their ability to replicate observed temperature, conclusions as to the generally performing models based on both studies is undeterminable. This is because, though some common models such as IPSL-CM6A-LR and MPI-ESM2-LR were found to have good performances as seen in (Ayugi et al., 2021b) for mean temperature and in this present study for minimum temperature. However, IPSL-CM6A-LR was found to be the second least ranking model for maximum temperature in this study. It is therefore not known whether similar ranking is obtainable if the same temperature classes are considered. Another factor that may affect the differences in results is the study region and the methods applied in the studies.

In evaluating the capability of twenty one CMIP6 GCMs in replicating daily precipitation during the West African Monsoon (WAM) period (June–September) over West Africa using three observations; Global Precipitation Climatology Project (GPCP), Climate Hazards Group InfraRed Precipitation (CHIRPS), and Tropical Applications of Meteorology (TAMSAT) datasets for validation of the model simulations, (Klutse et al., 2021) found that there are substantial discrepancies amongst the models and in comparison with the observations. It was concluded that there was no single model that exhibited all features of the observational datasets. Our findings show similarity to their study in that no GCM was able to completely replicate both the spatial and annual cycle of monthly precipitation or temperature. Apparently, this justifies the need for evaluation of models to select the most realistic ones or their aggregation into ensembles for projection of climate in order to reduce the individual uncertainties associated with different GCMs. However, this selection does not necessarily rank a GCM similar under different variables. For example, CMCC-CM2-SR5 which ranked high for precipitation had the least performances for the maximum and the minimum temperature. Similarly, INM-CM4-8 which ranked high for temperature showed a lower ranking for precipitation. This can be attributed to several factors including; the quality of the observed data (Miao et al., 2012), in which the observed climatological records may contain in-homogeneities; which can be as a result of factors such as changes in measurement practices, relocation of stations, and changes in a station's surroundings over the years (Ducré-Robitaille et al., 2003). The climatic condition and terrain of an area can also be a factor. A study conducted over the Tibetan Plateau (Lun et al., 2020) revealed significant differences in the simulation of some GCMs for different climatic variables. For example, CanESM5 from CMIP6 simulated precipitation (Rank Score (RS): 6.09) better than the air temperature (RS: 3.11) while for FIO-ESM of the CMIP5, there was significantly better performance of the air temperature (RS: 7.01) than the precipitation (RS: 1.59).

CP is one of the methods of selecting GCMs that have been found to be efficient in a number of studies. Raju et al. (2017) applied the method for the ranking of 36 maximum and minimum temperature GCMs of CMIP5 using three performance indicators namely, Pearson correlation coefficient (CC), NRMSE, and SS over India. The study found CP was efficient in aggregating ensemble of different combination of GCMs based on their different weights over 40 grid points of India. CP method was applied by (Sa'adi et al., 2019) for aggregation of scores obtained by 20 temperature GCMs of the CMIP5 at the Borneo Island of South East Asia. The results of the study showed four GCMs: FIO-ESM, MRI-CGCM3, GFDL-CM3, and IPSL-CM5A-MR as the most suitable ones for temperature projection over the region. Similarly, Ahmed et al. (2019) used the method to assess the performances of 20 precipitation and temperature GCMs of the CMIP5 over Pakistan. The study considered NRMSE, SS, and CC. The method identified CESM1-CAM5, HadGEM2-AO, NorESM1-M and GFDL-CM3 as the best performing GCMs for the area.

This study demonstrates the efficiency of CP method in the aggregation of ensemble GCMs based on the different statistical indicators which are sometimes contradictory. For example in precipitation, IPSL-CM6A-LR which has the best statistical score under NRMSE and NSE ranked 2nd for Pbias and 4th by R^2. This suggests the application of a robust approach such as CP can place all GCMs on a uniform assessment criterion. In addition, other applications using spatial performances, PDF curves, TD, and mean monthly precipitation to compare the GCMs with the observed have shown to be efficient as they all support the findings from the CP.

6. Conclusions

This study assesses the performances of 13 GCMs of the CMIP6 to replicate the properties of precipitation, maximum temperature and minimum temperature over Nigeria using five statistical indicators: NRMSE, Pbias, NSE, R^2, and VE; and the CP method. This was supplemented by spatial assessment, PDF plots, TD, and mean monthly precipitation assessments for the period 1984 – 2014. The study revealed that CP was able to uniformly evaluate the GCMs even though there were some contradictory results in the statistical indicators. Spatial assessment of the GCMs in relation to the observed show the highest ranked GCMs by the CP were able to better reproduce the properties of the GPCC precipitation and the CRU maximum and minimum temperatures. The least ranking GCMs, according to the CP were observed to have either spatially overestimate or underestimate precipitation and temperature over the study area. In combination with the other assessment methods, the GCMs were ranked using the final scores from the CP. For precipitation, IPSL-CM6A-LR, NESM3, CMCC-CM2-SR5, and ACCESS-ESM1-5 were the highest ranking GCMs. For maximum temperature, INM.CM4-8, BCC-CSM2-MR, MRI-ESM2-0, and ACCESS-ESM1-5 ranked the highest while for minimum temperature AWI-CM-1-1-MR, IPSL-CM6A-LR, INM.CM5-0, and CanESM5 ranked the highest. It is anticipated that the findings from this study are applied in the projection of climate using CMIP6 under different SSPs for Nigeria.

Conflicts of interests

The authors declare that they have no known competing interests that authors must disclose all affiliations, funding sources, financial or personal relationships that could be perceived as potential sources of bias.

Funding statement

This study was supported by National Research Foundation of Korea (2021R1A2C20056990).

Author contributions

Conceptualization, Mohammed Sanusi Shiru, and Eun-Sung Chung; Formal analysis, Mohammed Sanusi Shiru; Methodology, Mohammed Sanusi Shiru, and Eun-Sung Chung, Writing–original draft, Mohammed Sanusi Shiru, and Eun-Sung Chung; Writing – review & editing, Eun-Sung Chung,

Ethical approval

This article does not contain any studies with human or animal participants performed by any of the authors.

Availability of data and materials

The authors can support all relevant data if requested

Code Availability

The authors can support all relevant data if requested

Consent to Participate

The authors declare that they have consent to participate in this paper.

Consent to Publish

The authors declare that they have consent to publish in this journal.

References

Ahmed, K., Sachindra, D.A., Shahid, S., Demirel, M.C., Eun-Sung, C., 2019a. Selection of multi-model ensemble of general circulation models for the simulation of precipitation and maximum and minimum temperature based on spatial assessment metrics. Hydrology and Earth System Sciences 23, 4803-4824.

Ahmed, K., Shahid, S., Sachindra, D., Nawaz, N., Chung, E.-S., 2019b. Fidelity assessment of general circulation model simulated precipitation and temperature over Pakistan using a feature selection method. Journal of hydrology 573, 281-298.

Alamgir, M., Mohsenipour, M., Homsi, R., Wang, X., Shahid, S., Shiru, M.S., Alias, N.E., Yuzir, A., 2019. Parametric Assessment of Seasonal Drought Risk to Crop Production in Bangladesh. Sustainability 11, 1442.

Almazroui, M., Saeed, F., Saeed, S., Islam, M.N., Ismail, M., Klutse, N.A.B., Siddiqui, M.H., 2020a. Projected change in temperature and precipitation over Africa from CMIP6. Earth Systems and Environment, 1-21.

Almazroui, M., Saeed, S., Saeed, F., Islam, M.N., Ismail, M., 2020b. Projections of precipitation and temperature over the South Asian countries in CMIP6. Earth Systems and Environment 4, 297-320.

Asdak, C., Supian, S., 2018. Watershed management strategies for flood mitigation: A case study of Jakarta's flooding. Weather and climate extremes 21, 117-122.

Ayugi, B., Jiang, Z., Zhu, H., Ngoma, H., Babaousmail, H., Karim, R., Dike, V., 2021a. Comparison of CMIP6 and CMIP5 models in simulating mean and extreme precipitation over East Africa. International Journal of Climatology.

Ayugi, B., Ngoma, H., Babaousmail, H., Karim, R., Iyakaremye, V., Sian, K.T.L.K., Ongoma, V., 2021b. Evaluation and projection of mean surface temperature using CMIP6 models over East Africa. Journal of African Earth Sciences, 104226.

Ayugi, B., Tan, G., Rouyun, N., Zeyao, D., Ojara, M., Mumo, L., Babaousmail, H., Ongoma, V., 2020. Evaluation of Meteorological Drought and Flood Scenarios over Kenya, East Africa. Atmosphere 11, 307.

Babaousmail, H., Hou, R., Ayugi, B., Ojara, M., Ngoma, H., Karim, R., Rajasekar, A., Ongoma, V., 2021. Evaluation of the Performance of CMIP6 Models in Reproducing Rainfall Patterns over North Africa. Atmosphere 12, 475.

Becker, A., Finger, P., Meyer-Christoffer, A., Rudolf, B., Schamm, K., Schneider, U., Ziese, M., 2013. A description of the global land-surface precipitation data products of the Global Precipitation Climatology Centre with sample applications including centennial (trend) analysis from 1901–present. Earth System Science Data 5, 71-99.

Chen, F.-W., Liu, C.-W., 2012. Estimation of the spatial rainfall distribution using inverse distance weighting (IDW) in the middle of Taiwan. Paddy Water Environ 10, 209-222.

Chen, J., Brissette, F.P., Lucas-Picher, P., Caya, D., 2017. Impacts of weighting climate models for hydro-meteorological climate change studies. Journal of Hydrology 549, 534-546.

Diallo, I., Giorgi, F., Stordal, F., 2018. Influence of Lake Malawi on regional climate from a double-nested regional climate model experiment. Climate dynamics 50, 3397-3411.

Ducré-Robitaille, J.F., Vincent, L.A., Boulet, G., 2003. Comparison of techniques for detection of discontinuities in temperature series. International Journal of Climatology: A Journal of the Royal Meteorological Society 23, 1087-1101.

Eyring, V., Bony, S., Meehl, G.A., Senior, C.A., Stevens, B., Stouffer, R.J., Taylor, K.E., 2016. Overview of the Coupled Model Intercomparison Project Phase 6 (CMIP6) experimental design and organization. Geoscientific Model Development 9, 1937-1958.

Funk, C., Husak, G., Michaelsen, J., Love, T., Pedreros, D., 2007. Third generation rainfall climatologies: satellite rainfall and topography provide a basis for smart interpolation, Proceedings of the JRC—FAO Workshop, Nairobi, Kenya.
Gidden, M., Riahi, K., Smith, S., Fujimori, S., Luderer, G., Kriegler, E., van Vuuren, D.P., van den Berg, M., Feng, L., Klein, D., 2019. Global emissions pathways under different socioeconomic scenarios for use in CMIP6: a dataset of harmonized emissions trajectories through the end of the century. Geoscientific model development discussions 12, 1443-1475.
Grose, M.R., Narsey, S., Delage, F., Dowdy, A.J., Bador, M., Boschat, G., Chung, C., Kajtar, J., Rauniyar, S., Freund, M., 2020. Insights from CMIP6 for Australia's future climate. Earth's Future 8, e2019EF001469.
Gupta, H.V., Sorooshian, S., Yapo, P.O., 1999. Status of automatic calibration for hydrologic models: Comparison with multilevel expert calibration. Journal of hydrologic engineering 4, 135-143.
Harris, I., Jones, P.D., Osborn, T.J., Lister, D.H., 2014. Updated high-resolution grids of monthly climatic observations–the CRU TS3. 10 Dataset. International journal of climatology 34, 623-642.
Hausfather, Z., 2018. Explainer: How 'Shared Socioeconomic Pathways' explore future climate change. Carbon Brief 19.
Hawkins, E., Sutton, R., 2009. The potential to narrow uncertainty in regional climate predictions. Bulletin of the American Meteorological Society 90, 1095-1108.
Homsi, R., Shiru, M.S., Shahid, S., Ismail, T., Harun, S.B., Al-Ansari, N., Chau, K.-W., Yaseen, Z.M., 2020. Precipitation projection using a CMIP5 GCM ensemble model: a regional investigation of Syria. Engineering Applications of Computational Fluid Mechanics 14, 90-106.
Iqbal, Z., Shahid, S., Ahmed, K., Ismail, T., Nawaz, N., 2019. Spatial distribution of the trends in precipitation and precipitation extremes in the sub-Himalayan region of Pakistan. Theoretical and Applied Climatology, 1-15.
Johnston, K., 2004. ArcGIS 9: using ArcGIS geostatistical analyst. Esri Press.
Khan, N., Sachindra, D., Shahid, S., Ahmed, K., Shiru, M.S., Nawaz, N., 2020a. Prediction of droughts over Pakistan using machine learning algorithms. Advances in Water Resources 139, 103562.
Khan, N., Shahid, S., Ahmed, K., Wang, X., Ali, R., Ismail, T., Nawaz, N., 2020b. Selection of GCMs for the projection of spatial distribution of heat waves in Pakistan. Atmospheric Research 233, 104688.
Klutse, N.A.B., Quagraine, K.A., Nkrumah, F., Quagraine, K.T., Berkoh-Oforiwaa, R., Dzrobi, J.F., Sylla, M.B., 2021. The climatic analysis of summer monsoon extreme precipitation events over West Africa in CMIP6 simulations. Earth Systems and Environment 5, 25-41.
Knutti, R., Furrer, R., Tebaldi, C., Cermak, J., Meehl, G.A., 2010. Challenges in combining projections from multiple climate models. Journal of Climate 23, 2739-2758.
Legates, D.R., McCabe Jr, G.J., 1999. Evaluating the use of "goodness-of-fit" measures in hydrologic and hydroclimatic model validation. Water resources research 35, 233-241.
Lun, Y., Liu, L., Cheng, L., Li, X., Li, H., Xu, Z., 2020. Assessment of GCMs simulation performance for precipitation and temperature from CMIP5 to CMIP6 over the Tibetan Plateau. International Journal of Climatology.
Lutz, A.F., ter Maat, H.W., Biemans, H., Shrestha, A.B., Wester, P., Immerzeel, W.W., 2016. Selecting representative climate models for climate change impact studies: an advanced envelope-based selection approach. International Journal of Climatology 36, 3988-4005.
MacDonald, A., Cobbing, J., Davies, J., 2005. Developing groundwater for rural water supply in Nigeria: a report of the May 2005 training course and summary of groundwater issues in the eight focus states.
Manawi, S.M.A., Nasir, K.A.M., Shiru, M.S., Hotaki, S.F., Sediqi, M.N., 2020. Urban Flooding in the Northern Part of Kabul City: Causes and Mitigation. Earth Systems and Environment, 1-12.
Miao, C., Duan, Q., Yang, L., Borthwick, A.G., 2012. On the applicability of temperature and precipitation data from CMIP3 for China. PLoS One 7, e44659.

Moriasi, D.N., Arnold, J.G., Van Liew, M.W., Bingner, R.L., Harmel, R.D., Veith, T.L., 2007. Model evaluation guidelines for systematic quantification of accuracy in watershed simulations. Transactions of the ASABE 50, 885-900.

Nash, J.E., Sutcliffe, J.V., 1970. River flow forecasting through conceptual models part I—A discussion of principles. Journal of hydrology 10, 282-290.

Ngene, B.U., Agunwamba, J., Nwachukwu, B., Okoro, B., 2015. The Challenges to Nigerian Raingauge Network Improvement. Research Journal of Environmental and Earth Sciences 7, 68-74.

O'Neill, B.C., Tebaldi, C., Van Vuuren, D.P., Eyring, V., Friedlingstein, P., Hurtt, G., Knutti, R., Kriegler, E., Lamarque, J.-F., Lowe, J., 2016. The scenario model intercomparison project (ScenarioMIP) for CMIP6.

Onyutha, C., Tabari, H., Rutkowska, A., Nyeko-Ogiramoi, P., Willems, P., 2016. Comparison of different statistical downscaling methods for climate change rainfall projections over the Lake Victoria basin considering CMIP3 and CMIP5. Journal of hydro-environment research 12, 31-45.

Penalba, O.C., Rivera, J.A., 2016. Regional aspects of future precipitation and meteorological drought characteristics over Southern South America projected by a CMIP5 multi-model ensemble. International Journal of Climatology 36, 974-986.

Raju, K.S., Sonali, P., Kumar, D.N., 2017. Ranking of CMIP5-based global climate models for India using compromise programming. Theoretical and applied climatology 128, 563-574.

Rezaei, F., Ahmadzadeh, M.R., Safavi, H.R., 2017. SOM-DRASTIC: using self-organizing map for evaluating groundwater potential to pollution. Stochastic Environmental Research and Risk Assessment 31, 1941-1956.

Riahi, K., Van Vuuren, D.P., Kriegler, E., Edmonds, J., O'neill, B.C., Fujimori, S., Bauer, N., Calvin, K., Dellink, R., Fricko, O., 2017. The shared socioeconomic pathways and their energy, land use, and greenhouse gas emissions implications: an overview. Global Environmental Change 42, 153-168.

Rivera, J.A., Arnould, G., 2020. Evaluation of the ability of CMIP6 models to simulate precipitation over Southwestern South America: Climatic features and long-term trends (1901–2014). Atmospheric Research, 104953.

Sa'adi, Z., Shiru, M.S., Shahid, S., Ismail, T., 2019. Selection of general circulation models for the projections of spatio-temporal changes in temperature of Borneo Island based on CMIP5. Theoretical and Applied Climatology, 1-21.

Salman, S.A., Shahid, S., Afan, H.A., Shiru, M.S., Al-Ansari, N., Yaseen, Z.M., 2020. Changes in Climatic Water Availability and Crop Water Demand for Iraq Region. Sustainability 12, 3437.

Salman, S.A., Shahid, S., Ismail, T., Al-Abadi, A.M., Wang, X.-j., Chung, E.-S., 2019. Selection of gridded precipitation data for Iraq using compromise programming. Measurement 132, 87-98.

Samal, R.K., Kansal, M.L., 2015. Sustainable development contribution assessment of renewable energy projects using AHP and compromise programming techniques, 2015 International Conference on Energy, Power and Environment: Towards Sustainable Growth (ICEPE). IEEE, pp. 1-6.

Shiru, M., Shahid, S., Alias, N., Chung, E.-S., 2018. Trend analysis of droughts during crop growing seasons of Nigeria. Sustainability 10, 871.

Shiru, M.S., Chung, E.-S., Shahid, S., 2020a. Empirical Model for the Assessment of Climate Change Impacts on Spatial Pattern of Water Availability in Nigeria, Intelligent Data Analytics for Decision-Support Systems in Hazard Mitigation. Springer, pp. 405-427.

Shiru, M.S., Chung, E.-S., Shahid, S., Alias, N., 2020b. GCM selection and temperature projection of Nigeria under different RCPs of the CMIP5 GCMS. Theoretical and Applied Climatology 141, 1611-1627.

Shiru, M.S., Shahid, S., Chung, E.-S., Alias, N., Scherer, L., 2019a. A MCDM-based framework for selection of general circulation models and projection of spatio-temporal rainfall changes: A case study of Nigeria. Atmospheric Research 225, 1-16.

Shiru, M.S., Shahid, S., Dewan, A., Chung, E.-S., Alias, N., Ahmed, K., Hassan, Q.K., 2020c. Projection of meteorological droughts in Nigeria during growing seasons under climate change scenarios. Scientific reports 10, 1-18.

Shiru, M.S., Shahid, S., Shiru, S., Chung, E.S., Alias, N., Ahmed, K., Dioha, E.C., Sa'adi, Z., Salman, S., Noor, M., 2019b. Challenges in water resources of Lagos mega city of Nigeria in the context of climate change. Journal of Water and Climate Change.

Song, Y., Li, X., Bao, Y., Song, Z., Wei, M., Shu, Q., Yang, X., 2020. FIO-ESM v2. 0 Outputs for the CMIP6 Global Monsoons Model Intercomparison Project Experiments. Advances in Atmospheric Sciences, 1-12.

Sreelatha, K., Anand Raj, P., 2019. Ranking of CMIP5-based global climate models using standard performance metrics for Telangana region in the southern part of India. ISH Journal of Hydraulic Engineering, 1-10.

Tan, G., Ayugi, B., Ngoma, H., Ongoma, V., 2020. Projections of future meteorological drought events under representative concentration pathways (RCPs) of CMIP5 over Kenya, East Africa. Atmospheric Research, 105112.

Tanveer, M.E., Lee, M.-H., Bae, D.-H., 2016. Uncertainty and reliability analysis of CMIP5 climate projections in South Korea using REA method. Procedia engineering 154, 650-655.

Taylor, K.E., 2001. Summarizing multiple aspects of model performance in a single diagram. Journal of Geophysical Research: Atmospheres 106, 7183-7192.

Taylor, K.E., Stouffer, R.J., Meehl, G.A., 2012. An overview of CMIP5 and the experiment design. Bulletin of the American Meteorological Society 93, 485-498.

Tebaldi, C., Smith, R.L., Nychka, D., Mearns, L.O., 2005. Quantifying uncertainty in projections of regional climate change: A Bayesian approach to the analysis of multimodel ensembles. Journal of Climate 18, 1524-1540.

Tirivarombo, S., Osupile, D., Eliasson, P., 2018. Drought monitoring and analysis: standardised precipitation evapotranspiration index (SPEI) and standardised precipitation index (SPI). Physics and Chemistry of the Earth, Parts A/B/C 106, 1-10.

Willmott, C.J., 1982. Some comments on the evaluation of model performance. Bulletin of the American Meteorological Society 63, 1309-1313.

WMO, 1965. Guide to Hydro Meteorological Practice. World Meterological Organization, Geneva (In: Ngene, B.U., Agunwamba, J.C., Nwachukwu, B.A., and Okoro, B.C. (2015) The challenges to Nigerian rain gauge network improvement. Research Journal of Environmental and Earth Sciences 7(4): 68–74).

Xin, X., Wu, T., Zhang, J., Yao, J., Fang, Y., 2020. Comparison of CMIP6 and CMIP5 simulations of precipitation in China and the East Asian summer monsoon. International Journal of Climatology.

Zeleny, M., 1973. Compromise programming. Multiple criteria decision making.

Zhai, J., Mondal, S.K., Fischer, T., Wang, Y., Su, B., Huang, J., Tao, H., Wang, G., Ullah, W., Uddin, J., 2020. Future drought characteristics through a multi-model ensemble from CMIP6 over South Asia. Atmospheric Research, 105111.

Zhao, C., Jiang, Z., Sun, X., Li, W., Li, L., 2020. How well do climate models simulate regional atmospheric circulation over East Asia? International Journal of Climatology 40, 220-234.

Zhou, T., Chen, X., Wu, B., Guo, Z., Sun, Y., Zou, L., Man, W., Zhang, L., He, C., 2017. A robustness analysis of CMIP5 models over the East Asia-Western North Pacific domain. Engineering 3, 773-778.